Intercrossed Sheet-Like Ga-Doped ZnS Nanostructures with Superb Photocatalytic Actvitiy and Photoresponse

Ming-Yen Lu,[†,||] Ming-Pei Lu,[‡] Yao-An Chung,[†] Ming-Jer Chen,[§] Zhong Lin Wang,[||] and Lih-Juann Chen*[,†]

Department of Materials Science and Engineering, National Tsing Hua University, Hsinchu 30013, Taiwan R.O.C., National Nano Device Laboratories, Hsinchu, 30078, Taiwan R.O.C., Department of Electronics Engineering, National Chiao Tung University, Hsinchu, 30050, Taiwan R.O.C., School of Materials Science and Engineering, Georgia Institute of Technology, Atlanta, Georgia 30332-0245

Received: April 11, 2009; Revised Manuscript Received: May 16, 2009

Intercrossed ZnS nanostructures doped with Ga (ZnS:Ga nanowalls) have been synthesized in high yield from mixed powders in a vacuum furnace. ZnS:Ga nanowalls were grown vertically on the substrate with the size in the range of several micrometers and the thickness down to ~15 nm and have very rough edges. Due to the high surface area and distinctive morphology of ZnS:Ga nanowalls, the photocatalytic activity and the photoresponse show superior properties compared to ZnS:Ga films. The increased conductivity of metal−semiconductor−metal (Ag−ZnS:Ga nanowalls−Ag) Schottky photodetectors under light illumination is attributed to the photogenerated electron−hole pairs, the desorption of oxygen molecules on the ZnS:Ga surface, and the lowering of the Schottky barrier height. The results indicate that ZnS:Ga nanowalls are promising candidate materials for photocatalysts and applicable as photodetectors, optical switches, and sensors in the visible light region.

Introduction

Low-dimensional nanostructured materials have been successfully synthesized and have received much attention due to their importance in understanding the fundamental roles of dimensionality and quantum size effect and their potential applications serving as the building blocks for electronic,[1−3] optical,[4] and piezoelectric[5] nanodevices.

Zinc sulfide (ZnS) is an important II−IV semiconducting material with a wide bandgap energy of 3.7 eV and a large exciton binding energy (~40 meV). Due to its excellent properties of luminescence and photochemistry, its nanostructures have been studied extensively and reported in recent years. In addition to nanowires,[6,7] nanobelts,[8] and nanoparticles,[9] some fascinating morphologies have been reported.[10−12] Optoelectronics-related properties of nanostructures may depend sensitively on their structures, morphologies and sizes.[13,14] Often, they demonstrate significant effects, which are not the case for bulk materials. On the other hand, ZnS can also serves as an important semiconductor photocatalyst to remove organic or toxic water pollutants owing to the rapid generation of electron−hole pairs and the highly negative reduction potentials of excited electrons.[14]

In this paper, we report intercrossed sheet-like ZnS nanostructures with Ga dopant (ZnS:Ga nanowalls) grown on Si substrates by thermal evaporation of the mixed powders of ZnS and Ga_2O_3 via a self-catalyzed growth mechanism. Both the photocatalytic activity and photoresponse of ZnS:Ga nanowalls show superior properties due to its distinctive morphology and high surface areas.

* Corresponding author. E-mail: ljchen@mx.nthu.edu.tw. Phone: 886-35731166. Fax: 886-35718328.
[†] National Tsing Hua University.
[||] Georgia Institute of Technology.
[‡] National Nano Device Laboratories.
[§] National Chiao Tung University.

Experimental Section

Synthesis of Ga-Doped Nanowalls. Growth of ZnS:Ga nanowalls was carried out by thermal evaporation of mixed powders under controlled conditions. An alumina tube was mounted horizontally inside a tube furnace. A mixture of powders with different ratios of ZnS, Ga_2O_3 powders, and relative amounts of graphite as the source was placed in an alumina boat located at the high temperature zone. The Si (001) substrate was ultrasonically cleaned for 10 min in acetone. The substrate was positioned 15 cm away from the source at downstream (temperature = ~670 °C). After the tube had been sealed and evacuated to a pressure of 8×10^{-2} torr, a carrier gas of 100 sccm 95% Ar + 5% H_2 was kept flowing through the tube. During the deposition, pressure inside the tube was kept at 5.7 Torr. The ZnS powder source was heated at a rate of 10 °C /min to 1150 °C and kept for 15 min, 30 min, and 1 h. After depositions, the samples were cooled to room temperature in the furnace.

Morphology and Structure Characterization. The morphologies, chemical compositions and structures of the products were characterized by X-ray diffractometry (XRD, Shimadzu 6000-XRD) with Cu Kα radiation ($\lambda = 0.154$ nm), transmission electron microscopy (TEM, JEOL JEM-2010) and field-emission scanning electron microscopy (FESEM, JEOL JSM-6500F). Both SEM and TEM are equipped with an energy dispersive X-ray spectrometer (EDS) to analyze the chemical compositions of nanostructures.

Photocatalytic Activity Measurement. The photocatalytic activity of samples was examined by the degradation of methylene blue (MB) solution at room temperature. A piece of ZnS: Ga nanowall film with the size of 5 mm × 10 mm was placed at the sidewall inside the test bottle containing 8 mL of 28 mM methylene blue solution and stirred in the dark for 20 min to ensure the establishment of absorption equilibrium

10.1021/jp903350x CCC: $40.75
Published on Web 06/19/2009

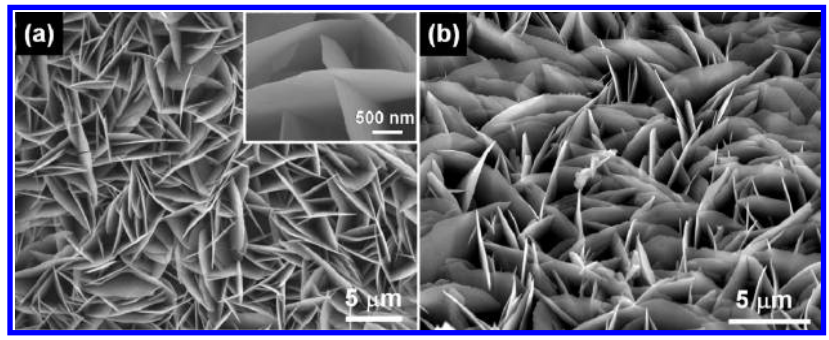

Figure 1. (a) Typical SEM image of ZnS:Ga nanowalls. The inset in panel a is a high magnification SEM image showing the nanowalls as thin as 15 nm. (b) The tilted SEM image of the ZnS:Ga nanowalls.

between the MB solution and catalysts. The top surface of samples was irradiated with the light from a 10 W UV lamp along the normal direction at a distance of about 7 cm under continuous stir. Commercial P25 TiO_2 films were adopted as the references with which to compare the photocatalytic activity of ZnS: Ga films under the same experimental condition. The concentration of MB solution was monitored by UV−vis spectrophotometer at various stages. One mL solution was used for UV−vis analysis at each stage. After the measurement, the solution in the test cell was poured back to the reaction solution and continued the photoexposure to make sure the exposed solution was of a constant volume of 8 mL.

Temperature Dependence I−V Measurement. ZnS:Ga nanowall photodetectors were built by placing Ag paste at the two ends of ZnS:Ga nanowall film as electrodes. The samples were then placed on the hot plate. When the temperature reached the set value, I−V measurements were carried out using a Semiconductor Characterization System (Keithley 4200).

Photoresponse Measurement. To characterize their photoresponse, the illumination was introduced from visible light of an optical microscope objective lens. The photocurrents and photoresponses were recorded with a HP 4156C Semiconductor Parameter Analyzer. All experiments are performed at room temperature in air.

Results and Discussion

2.1. Structural Characterization. ZnS:Ga nanowalls have been synthesized in high yield with the ratio of Ga_2O_3 and ZnS powders at 1:5, heated to 1150 °C, and kept for 1 h in the vacuum furnace. Figure 1a shows a SEM image of the as-deposited products on Si substrate. The products consist of a large quantity of sheet-like nanostructures with typical size in the range of several micrometers. The inset of Figure 1a is a high magnification SEM image showing that the sheets are as thin as 15 nm in thickness and have rough edges. The tilted SEM image of the structures is given in Figure 1b, which displays vertical morphology of the sheets, named nanowalls. Moreover, protruded islands of ZnS:Ga networks were formed for the short synthesis time (see Figure 1S, Supporting Information). It is important to clarify the role of Ga atoms in the synthesis. As Ga atoms take part in the reaction, the morphology of ZnS shows great difference and ZnS:Ga nanowalls come into existence (see Figure 2S, Supporting Information). With the increase in amount of Ga_2O_3 powders, ZnS:Ga nanowalls became more vertical and its edges became sharper. If the amount of Ga_2O_3 powders exceeded the critical quantity (Ga_2O_3:ZnS = 1:5), the morphology of ZnS:Ga nanowalls changed gradually from nanowalls to films.

X-ray diffraction patterns were used to determine the crystal structure and phase of ZnS:Ga nanowalls. An example is

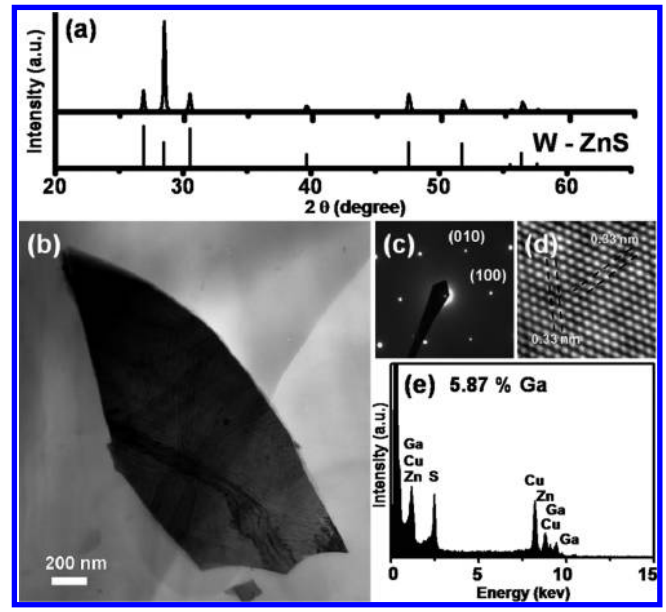

Figure 2. (a) XRD spectrum of the nanowalls. Standard XRD pattern for the hexagonal phase of ZnS is also shown. (b) Bright-field TEM image of a single ZnS:Ga nanowall. (c) The corresponding SAED taken from the nanowall. (d) HRTEM image of nanowall showing a perfect wurtzite structure with a [0001] zone axis. (e) EDS spectrum indicating the nanwalls are composed of Zn, S and Ga.

presented in Figure 2a. Only peaks due to the hexagonal wurtzite structure of ZnS with the lattice constant $a = 0.318$ nm, $c = 0.6260$ nm (JCPDS file: 89−2942) were detected from the XRD pattern. Figure 2b shows the bright-field TEM image of a single nanowall. The selected area electron diffraction pattern (SAED) taken from the nanowall is shown in Figure 2c indicating that the nanowall yields to one set of diffraction spots, corresponding to wurtzite-structured ZnS. The nanowalls are single crystalline and the *c* axis is perpendicular to the nanowalls. The HRTEM image given in Figure 2d shows a perfect wurtzite structure with a [0001] zone axis. The EDS spectrum is shown in Figure 2e. Analysis of spectra obtained by EDS indicated that the nanowalls are composed of Zn, S, and Ga. The Ga signal in Figure 2e represents the dopant in the presence study. The average molar fraction of Ga of ZnS:Ga nanowall is about 5.87%.

The observed ZnS:Ga nanowalls were apparently not grown via vapor−liquid−solid (VLS) mechanism, which has been the favored growth mode of nanostructures, because no catalysts were used. It is supposed that ZnS:Ga nanowalls were grown vertically from Si substrates via a combined mechanism. Because of the high evaporation temperature (1150 °C) of starting materials, the supersaturation of vapors is very high at first, which leads to the formation of polycrystalline ZnS:Ga

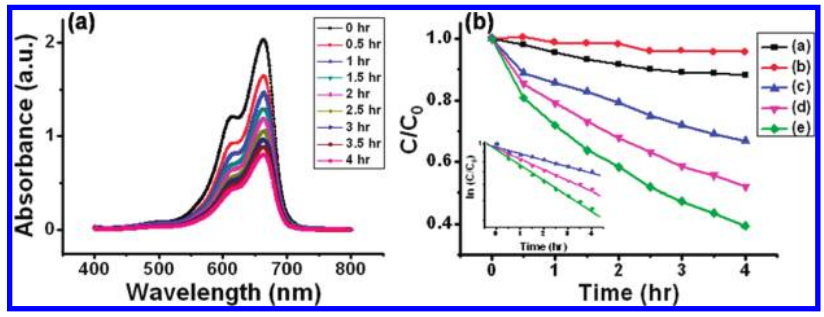

Figure 3. (a) Absorption spectrum of MB solution in the presence of ZnS:Ga nanowalls under exposure to UV light for various durations. The decrease in the intensity of absorbance peaks at 664 nm is attributed to the decomposition of the MB. (b) Variation with time of photodegradation of methylene blue under different conditions: (a) ZnS:Ga nanowalls, dark, (b) without catalysts, under UV light, (c) ZnS:Ga film, under UV light, (d) P25 TiO_2 film, under UV light, (e) ZnS:Ga nanowalls, under UV light. The inset of Figure 4b shows the data plotted into logarithmic scale. The data fit well to the equation of first order reaction kinetics.

film on silicon substrate. The film may act as a buffer layer, whereby nucleation occurs at the grain boundaries of the polycrystalline film via a vapor-solid mechanism. Furthermore, the lattice mismatch between wurtzite-ZnS film and Si substrate is very large; this favors the Volmer−Weber growth, which results in three-dimensional clusters at the early stage of growth.[15,16] Thus, ZnS:Ga nanowalls may grow at the grain boundaries of polycrystalline ZnS film. With the increase of synthesis time, the supply of vapors is gradually decreasing. Accordingly, ZnS:Ga nanowalls become thinner.

2.2. Photocatalytic Activities. The potential applicability of nanowalls was partially demonstrated by evaluating the photocatalytic activity of samples toward the photodegradation of 28 mM methylene blue (MB) using 10 W UV lamp as a light source. Samples with the same size were exposed along the normal direction and immersed in the solution under continuous stir. Figure 3a is the absorption spectrum of MB solution in the presence of ZnS:Ga nanowalls under exposure to UV light for various durations. The decrease in the intensity of absorbance peaks at 664 nm is attributed to the decomposition of the MB. A further comparative experiment was performed to investigate the photocatalytic activity of different samples (Figure 3b). Compared to the slight decrease in concentration of MB in the presence of ZnS:Ga nanowalls in the dark and without catalysts under UV light, ZnS:Ga film, P25 TiO_2 film as well as ZnS:Ga nanowalls exhibit remarkable decrease in absorbance under identical conditions. Commercial P25 TiO_2 has usually been used as a reference in the photocatalytic activity test. This decay behavior can be assumed as first order reaction kinetics

$$\ln[A(t)/A(0)] = -kt \qquad (1)$$

where k and t are the rate constant of this decay reaction and reaction time, respectively. The inset of Figure 3b shows the data plotted into logarithmic scale. The data were found to fit well to the equation and the rate constants are calculated. Ga:ZnS nanowalls show much greater activity than that of ZnS:Ga and P25 TiO_2 films. The superior photocatalytic property of ZnS:Ga is correlated to the large surface area. Although other factors such as the bandgap and crystallization can also affect photocatalytic activity of semiconductors, there are indications that the effects are not significant. CL spectra of ZnS:Ga nanowalls and film (not shown) do not show much difference. In addition, both the thin film and the nanowalls are crystalline. High photocatalytic efficiency of ZnS:Ga nanowalls is therefore attributed to its large surface area.

2.3. Temperature Dependent Current−Voltage Measurements. The typical current−voltage (I−V) curves of metal−semiconductor−metal (Ag−ZnS:Ga nanowalls−Ag; MSM) photodetectors were obtained at room temperature as shown in Figure 4a. It is well known that the different Schottky barrier heights between two metal-semiconductor (MS) contacts contribute to the nonlinear and asymmetrical current characteristics of photodetectors. The band diagram of metal−ZnS−metal structure under zero bias with different barrier height is shown in the inset of Figure 4a. Figure 4b is the I−V characteristics of ZnS:Ga nanowall MSM photodetectors measured at different temperatures between 300 and 448 K. It is demonstrated that the measured current is increased with temperature. The thermionic emission is the dominant transport mechanism in Schottky contact. The MSM photodetector has two Schottky barriers, one in the forward direction and the other in the reverse direction. Most of potential drops are at the reverse junction and the Schottky barrier heights at the reverse junction can be measured. The $\ln(I/T^2)$ versus $1/T$ at $V = +1$ and -1 V are shown in the inset of Figure 4b, and the effective Schottky barrier heights are extracted as 0.16 and 0.39 eV, respectively. The Schottky barrier height depends not only on the difference

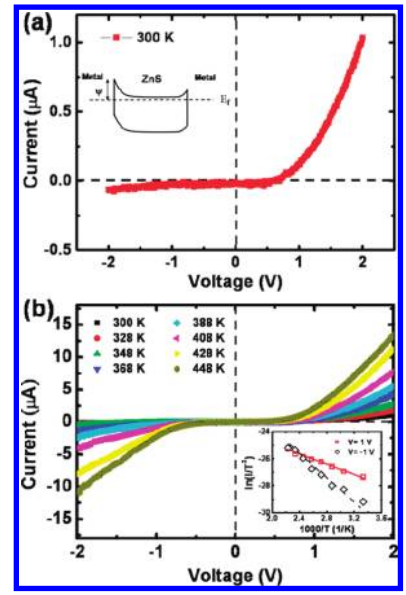

Figure 4. (a) Typical current−voltage curves of ZnS:Ga nanowall metal−semiconductor−metal (MSM) photodetectors measured at room temperature. The inset shows the band diagram of metal−ZnS−metal with different Schottky barrier heights at two contacts under zero bias. Ψ is the Schottky barrier height at metal/ZnS interface. (b) The temperature dependent I−V characteristics of ZnS:Ga nanowall MSM photodetectors measured at temperatures between 300 and 448 K.The inset is the plot of $\ln(I/T^2)$ versus $1/T$ at $V = +1$ and -1 V and the effective Schottky barrier heights are extracted as 0.16 and 0.39 eV, respectively.

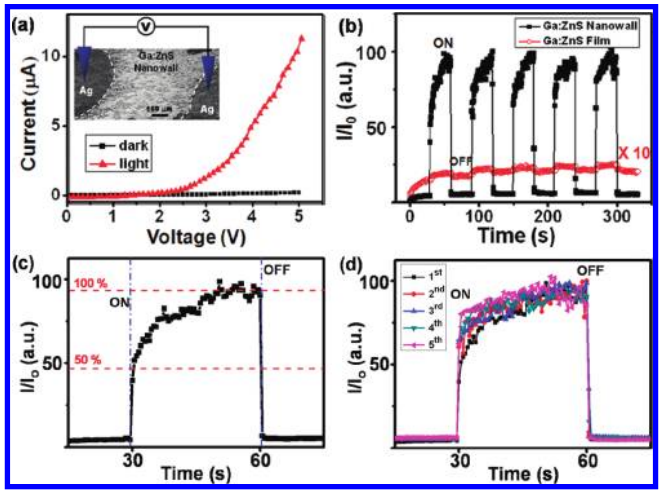

Figure 5. (a) Current−voltage (I−V) curves of ZnS:Ga nanowall photoconductor measured in the dark and upon light illumination with a sweep voltage from 0 to 5 V. The inset is a schematic illustration of ZnS:Ga nanowall photoconductor configuration. (b) The photoresponse of ZnS:Ga nanowall (black square line) and film (red circle line) for five cycles. Each interval is 30 s. I_0 is the dark current at $T = 0$ s. (c) The detailed photoresponse of a single cycle, indicating the fast response and recovery time of ZnS:Ga nanowalls. (d) The combined photoresponse curves showing the consistency for different cycles.

of work function between the metal electrode and semiconductor but also on the Fermi level pinning effect by surface states. Even the contaminations and molecules adsorbed at the MS interface will affect the Schottky barrier height. To clarify the cause for the difference in Schottky barrier height in the forward direction and reverse direction, further investigation is needed.

2.4. Photoconductive Properties. Figure 5a shows the current−voltage curves of ZnS:Ga nanowall photodetectors measured in the dark and upon light illumination with a sweep voltage from 0 to 5 V. It can be seen that the conductivities of ZnS:Ga nanowalls are rather small in the dark, but show a remarkable increase in conductance of up to 2 orders of magnitude upon the illumination of light. The inset of Figure 5a is a schematic illustration of ZnS:Ga nanowall photoconductor configuration showing that two electrodes are successfully made by placing Ag paste at two ends of ZnS:Ga nanowall film with a distance of about 550 μm. The enhanced conductivity during illumination is owing to the photogenerated electron−hole pairs and the desorption process of oxygen molecules on the surface. In the dark state, the oxygen molecules were adsorbed on the nanowall surface by grabbing free electrons from ZnS, therefore creating a depletion layer near the nanowall surface. On the other hand, holes with an equal amount as photoexcited electrons migrate to the surface to recombine with adsorbed oxygen ions in the illumination state. At the same time, the trapped electrons are released from the surface. Thus, the depletion width will be decreased and the total number of carriers is increased. The conductivity then significantly increases.[17] Moreover, the back-to-back forward and reverse Schottky barrier may play an important role in increasing the conductivity of ZnS: Ga photodetectors. The photoexcited charge accumulation at surface states leads to the lowering of the Schottky barrier height upon the light illumination and consequently the current increases.[18,19]

The photoresponse of ZnS:Ga nanowall photodetectors (black square line) as a function of time is plotted in Figure 5b. In Figure 5b. The current was measured at a constant bias of 5 V while the light-illuminated state as "ON" and the dark state as "OFF". The measurements are repeated with 30 s interval for five cycles. It can be seen that the switching between "ON" and "OFF" states is reversible and the ON/OFF ratio of photodetectors is about 100 and all illuminating processes are reproducible. The detailed photoresponse of a single cycle is plotted in Figure 5c. The current increased rapidly to 50% of maximum value within 1 s and then slowly reached the saturation value within 25 s at light-illuminated state. After the light was turned off, the current drastically recovered to the original value within 0.5 s. Since 0.5 s is the interval between two neighboring data points and also the detection limit of measurement system, it is very likely that the recovery time was less than 0.5 s. It is worth noticing that the recovery time is faster than the response time, which is due to the difference of adsorption and desorption rate of oxygen molecules on ZnS:Ga nanowall's surface.[20] Moreover, both of the response and recovery time in our work are comparable with single ZnS nanobelts.[21] Figure 5d shows the combined photoresponse curves which is acquired from Figure 5b. The consistent trends of curves indicate the same photoexcited mechanism and reveal the repeatability of each cycle. The other photoresponse curve (red circle line) plotted in Figure 5b is recorded with ZnS:Ga film (Figure S1b, Supporting Information). It can be clearly seen that the sensitivity (ON/OFF ratio) of ZnS:Ga nanowalls is up to three orders in magnitude higher than it of ZnS:Ga film, which is attributed to the high surface area to volume ratio of ZnS:Ga nanowalls. Due to the effect of high surface area, the photoresponse of ZnS:Ga nanowalls not only demonstrates the high sensitivity, but shows rapid response and recovery, as well as the reversibility.

Summary and Conclusions

To summarize, by using a simple vapor-transport deposition method, ZnS nanowalls with Ga dopants have been successfully synthesized. Intercrossed sheet-like ZnS:Ga nanostructures are grown vertically via a combined mechanism on the polycrystalline ZnS:Ga films. The incorporation of Ga ions into the ZnS resulted in morphological changes. ZnS nanowalls doped with Ga ions show superior results of photocatalytic properties, photoresponse as well. The increasing conductivities of ZnS:Ga MSM Schottky photodetectors under light illumination are owing to the photogenerated electron−hole pairs, the desorption of oxygen molecules on ZnS:Ga nanowall surface and the lowering of Schottky barrier height. The results indicate that ZnS:Ga nanowalls are promising candidate materials systems as photocatalysts and applicable as photodetectors, optical switches and sensors in visible light region.

Acknowledgment. The authors acknowledge the support of the ROC National Science Council through Grant No. NSC 97-2120-M-007-003.

Supporting Information Available: SEM images of samples synthesized with different time and different ratios of Ga_2O_3 and ZnS powders are shown in Figures S1 and S2, respectively. This material is available free of charge via the Internet at http://pubs.acs.org.

References and Notes

(1) Cui, Y.; Lieber, C. M. *Science* **2001**, *291*, 851–853.
(2) Chen, L. J. *J. Mater. Chem.* **2007**, *17*, 4639–4643.
(3) Lin, Y. C.; Lu, K. C.; Wu, W. W.; Bai, J. W.; Chen, L. J.; Tu, K. N.; Huang, Y. *Nano Lett.* **2008**, *8*, 913–918.
(4) Noda, S.; Tomoda, K.; Yamamoto, N.; Chutinan, A. *Science* **2000**, *289*, 604–606.
(5) He, J. H.; Hsin, C. L.; Liu, J.; Chen, L. J.; Wang, Z. L. *Adv. Mater.* **2007**, *19*, 781–784.

(6) Zhu, Y. C.; Bando, Y.; Xue, D. F.; Golberg, D. *Adv. Mater.* **2004**, *16*, 831–834.
(7) Lu, M. Y.; Song, J.; Lu, M. P.; Lee, C. Y.; Chen, L. J.; Wang, Z. L. *ACS Nano* **2009**, *3*, 357–362.
(8) Wang, Z. W.; Daemen, L. L.; Zhao, Y. S.; Zha, C. S.; Downs, R. T.; Wang, X. D.; Wang, Z. L.; Hemley, R. J. *Nat. Mater.* **2005**, *4*, 922–927.
(9) Chen, W.; Wang, Z. G.; Lin, Z. J.; Lin, L. Y. *J. Appl. Phys.* **1997**, *82*, 3111–3115.
(10) Ma, C.; Moore, D.; Li, J.; Wang, Z. L. *Adv. Mater.* **2003**, *15*, 228–231.
(11) Lu, M. Y.; Su, P. Y.; Chueh, Y. L.; Chen, L. J.; Chou, L. J. *Appl. Sur. Sci.* **2005**, *244*, 96–100.
(12) Deng, Z.; Qi, J.; Zhang, Y.; Liao, Q.; Huang, Y. *Nanotechnology* **2007**, *18*, 475603.
(13) Tien, L.; Sadik, P.; Norton, D. P.; Voss, L.; Pearton, S. J.; Wang, H. T.; Kang, B. S.; Ren, F.; Jun, J.; Lin, J. *Appl. Phys. Lett.* **2005**, *87*, 222106.
(14) Hu, J. S.; Ren, L. L.; Guo, Y. G.; Liang, H. P.; Cao, A. M.; Wan, L. J.; Bai, C. L. *Angew. Chem., Int. Ed.* **2005**, *44*, 1269–1273.
(15) Floro, J. A.; Hearne, S. J.; Hunter, J. A.; Kotula, P.; Chason, E.; Seel, S. C.; Thompson, C. V. *J. Appl. Phys.* **2001**, *89*, 4886–4897.
(16) Zhang, B. P.; Binh, N. T.; Wakatsuki, K.; Segawa, Y.; Yamada, Y.; Usami, N.; Kawasaki, M.; Koinuma, H. *J. Phys. Chem. B* **2004**, *108*, 10899–10902.
(17) Kind, H.; Yan, H.; Messer, B.; Law, M.; Yang, P. *Adv. Mater.* **2002**, *14*, 158–160.
(18) Bum, J.; Eastman, L. F. *IEEE Photonics Technol. Lett.* **1996**, *8*, 113–115.
(19) Behnam, A.; Johnson, J.; Choi, Y.; Noriega, L.; Ertosun, M. G.; Wu, Z.; Rinzler, A. G.; Kapur, P.; Saraswat, K. C.; Ural, A. *J. Appl. Phys.* **2008**, *103*, 114315.
(20) Chueh, Y. L.; Hsieh, C. H.; Chang, M. T.; Chou, L. J.; Lao, C. S.; Song, J. H.; Gan, J. Y.; Wang, Z. L. *Adv. Mater.* **2007**, *19*, 143–149.
(21) Liu, Y. G.; Feng, P.; Xue, X. Y.; Shi, S. L.; Fu, X. Q.; Wang, C.; Wang, Y. G.; Wang, T. H. *Appl. Phys. Lett.* **2007**, *90*, 042109.

JP903350X